

Prediction of moment capacity of ferrocement composites with chicken mesh and steel slag using response surface methodology and artificial neural network

Ramasamy Maguteeswaran¹ , Jayaprakash Sridhar², Rajendiran Gangadevi³, Natarajan Malathi⁴, Moorthy Sujatha⁵, Vivek Sivakumar²

¹Suguna College of Engineering, Department of Mechanical Engineering, Coimbatore, Tamil Nadu, India.

²GMR Institute of Technology, Department of Civil Engineering, Rajam, Andhra Pradesh, India.

³SRM Institute of Science and technology, Department of Mechatronics Engineering, Kattankulathur, Tamil Nadu, India.

⁴Saveetha University, Saveetha School of Engineering, Saveetha Institute of Medical and Technical Sciences, Department of Computer Science and Engineering, Chennai, Tamil Nadu, India.

⁵Koneru Lakshmaiah Education Foundation, Department of Electronics and Communication Engineering, Vijayawada, Andhra Pradesh, India.

e-mail: magu999@gmail.com, sridharjayaprakash@gmail.com, gangader@srmist.edu.in, malathigopinath@yahoo.co.in, sujakarthik77@kluniversity.in, vivek.s@gmrit.edu.in

ABSTRACT

In the present study, Response Surface Methodology model (RSM) and Artificial Neural Network model (ANN) is presented to forecast the ultimate moment capacity of ferrocement using 2 variable process modelling (volume fraction and steel slag replacement). The RSM and ANN model's outcomes are contrasted with those of other existing models, like plastic analysis, mechnaism approcah, simplified method, group method of data handling, the results shows that ferrocement with steel slag replacement of 25% and chicken mesh volume fraction (V_p) of 4.35% has maximum experimental moment capacity of 253.33 kN-mm and predicted moment capacity using RSM and ANN is 244.70 kNmm and 255.88 kNmm respectively. The adopted ANN have a regression value of 0.9882 and 0.98863 for training and testing respectively. The outcomes of the analysis of variance show that the provided models are very suitable since the p value is less than 0.005, the projected R2 and the adjustable R2 is less than 20%. Moreover, the flexural moment of ferrocement composites is more significantly affected by the V_p . According to the findings of the surface plot, Pareto chart, and regression analysis, the V_p is the most important and crucial factor for the flexural moment of ferrocement composites.

Keywords: Steel slag; Ferrocement; Artificial Neural network; Leven Berg-Marquardt; Response Surface Methodology.

1. INTRODUCTION

The need for cement and concrete will therefore continue to rise due to the expected urbanisation over the next 50 to 100 years, necessitating initiatives to lessen their environmental impact. Current engineering techniques are continually pushing for the improvement of ultra-high performance multifunctional building materials [1]. These materials must exhibit enhanced durability and mechanical performance, as well as numerous functionalities, to be suitable for new structural applications. Researchers agree that improving concrete's chemical and physio mechanical properties requires working at the micro scale. Ferrocement composite is one of the answers to that perennial problem which enhances many properties of concrete and mortar [2] Ferrocement composite (FC) is a reinforced concrete construction material which is produced with galvanised or non-galvanised mesh. As 90% of its total volume FC is mortar the quality of mortar matrix and its composition has a vital role in the behaviour of ferrocement composites [3]. The behaviour of materials contained in ferrocement is determined by orientation, the strength of the mesh, and the reinforcing rods. Its ultimate strength is determined by the volume fraction of mesh reinforcement [4, 5]. Theoretical predictions support the experimental findings for chicken mesh ferrocement with skeleton reinforcement as bamboo and a plaster mixture of 1:3.5 [6]. Lightweight ferrocement beams with extended metal mesh have developed post cracking load when compared with weld mesh [7].

Load carrying capacity of ferrocement with galvanized iron mesh (GI) and polypropylene (PP) mesh increases with volume fraction, whereas PP mesh exhibits better ductility when compared with GI meshes [8]. Ferrocement panels with volume fraction 2.35% and 3.77% and 30% steel slag substitution for sand has ultimate load maximum energy absorption when compared conventional panels under Impact load [9, 10]. The axial stress increases by sixty one percent and thirty one percent correspondingly for ferrocement containing 2 and 4 layers of weld mesh with cement matrix containing metakaolin and silica fumes [11]. The strength of RC beams is enhanced under flexure with use of weld mesh composites when compared with beams strengthened with carbon fibers [12]. Strengthening of reinforced concrete ferrocement with more layers of wire mesh produce better yield loads, ultimate loads, and stiffnesses [13]. Ferrocement panels with High calcium wood ash (HCWA) up to 40% exhibited superior performance as compared to panels without HCWA [14]. Flexural capacity and energy absorption rises with the rise in number of layers of mesh while the crack width decreases [15]. Higher ultimate loads, yield loads and stiffness are achieved as the number of layers are increased in ferrocement laminates [13]. Accuracy of the forecast moment capacity with self-evolving network model of the ferrocement is more with that of the existing models [16]. When compared to other models, the Group Method of Data Handling (GMDH) has a complex accuracy for predicting the ultimate moment capacity of ferrocement [17]. Comparing to other models like the plastic analysis technique, Mechanism approach method, Simplified method, GEP models, and GMDH models, the ultimate moment capacity predicted by the back-propagation multilayer perceptron artificial neural network has superior accuracy. As related to other approaches like GMDH and ANFIs, the predictable ultimate moment of ferrocement using ANN has a higher level of accuracy [18].

Digital image correlation used to characterize ferrocement laminates shows that as no of mesh layers increases flexural capacity and energy absorption increases while fracture width reduces [19]. Concrete slabs with chicken mesh reinforcement and bamboo skeleton reinforcement exhibit higher mechanical qualities, and theoretical predictions complement the experimental findings [15]. Design of Experiments (DOE) statistical and mathematical approach, ideally Response Surface Methodology, may be used to study the influence of the independent variables on the results with the least trials [20–23]. DOE may be used to optimize the test variables and produces the best outcome for experimental data as creates good bond between independent variables and empirical model [24]. Radial Basis Function Neural Network (RBFNN) outperformed the Multiple Linear Regression (MLR) in simulating the removal of hydrochlorothiazide (HCT) by two adsorbents. The optimal RBFNN model, when tested with the dataset, demonstrated strong predictive capabilities for HCT removal (%), yielding coefficient of determination (R^2) values of 0.8460 and 0.9438 for multi-walled carbon nanotubes (MWCNTs) and single-walled carbon nanotubes (SWCNTs), respectively. The corresponding mean squared error (MSE) values were 0.0117 for SWCNTs and 0.0010 for MWCNT [25]. The regression analysis model developed using RSM to predict compressive strength and split tensile strength of concrete containing natural fibres demonstrates a close agreement between the forecasted values and the experimental results [26]. The artificial neural network (ANN) model demonstrates effective predictive performance. In the constructed models, the predicted values closely align with the experimental data for both training and testing sets. The anticipated values generated by the adaptive neuro-fuzzy inference system (ANFIS) model were highly accurate. Additionally, a comparison of performance indices indicates that the ANFIS model outperformed the ANN model to some extent [27]. The main in this study is to predict the moment capacity of ferrocement composites with chicken mesh and steel slag using RSM and ANN and to develop accurate and reliable models that can forecast the structural performance of these composites under various conditions. In the present study, the moment capacity of ferrocement with steel slag and chicken mesh was predicted using CCM in RSM and ANN Feed-forward back propagation neural network NN-LM using ANN base model. The DOE approach and ANN are used to analyze the trial findings in order to find the best grouping of the self-governing variables (V_r and steel slag). Moreover, feed-forward back propagation neural networks and Leven Berg-Marquardt (NN-LM) neural networks were used as training functions for ANN. In order to assess the efficacy of each strategy, root mean square error (RMSE), the coefficient of determination (R^2), mean absolute error (MAE), mean square error (MSE) and mean absolute and percentage error (MAPE) of the two models were contrasted. By combining RSM, which is effective in exploring complex relationships among multiple factors, with ANN, renowned for its ability to capture intricate non-linear patterns, this study achieves a comprehensive understanding of the moment capacity. The utilization of chicken mesh and steel slag as composite materials introduces innovative elements, contributing to the optimization of ferrocement structures. This approach not only improves prediction accuracy but also provides insights into the synergistic effects of these materials, fostering advancements in the design and analysis of ferrocement composites for improved structural efficiency.

2. MATERIALS AND METHODS

2.1. Mathematical models

2.1.1. Response surface method

Response Surface Methodology (RSM) is a numerical technique used for optimizing and analysing complex processes. It involves designing experiments, collecting data, and creating mathematical models to describe the relationship between input variables and the output response. The optimal experimental conditions can be improved with the help of response surface optimisation. Response Surface Methodology successfully optimises trials by taking into consideration both statistical and mathematical approaches for analysis in order to compute the total number of experimental data for better performance. When there are several variables, RSM can be used to look at how each one affects the others and how they interact, as well as how important each variable is to the responses or models [28]. To ascertain the association between outcome variables and independent factors in RSM, central composite design is employed [29]. Factors and levels of variables must be given for the examined responses as shown in Table 1 for DOE of RSM autonomous variables. By applying Equation 1 the necessary number of experiments is determined.

$$N = 2^y + 2y + n \quad (1)$$

where n = number of centre points and y = number of components [30].

2.1.2. Artificial Neural Network

The Artificial Neural Network (ANN) is a computational framework that consists of input layers, hidden layers, and output layers. It has been extensively validated as an effective prediction method for accurately forecasting output variables in various models. The key benefit of utilizing ANN is its capacity to accurately model complex, non-linear relationships with multiple input variables. Additionally, ANN tools are highly favoured due to their capability to handle inconsistent and unreliable data, as well as their resilience and fault tolerance [30, 31]. The effectiveness of present ANN model depends on 2 input neurons, 1 output neurons, 6 hidden layers and activation function.

- (i) Inside the input layer, there are three neurons ($N_i = 3$) that represent the volume fraction of weld mesh V_r (%), steel slag (% by weight of FA).
- (ii) In output layer vegetative cell denotes the value of the ultimate moment capacity.
- (iii) Six Neurons are available in the hidden layers.

The neurons are bourgeoned by the respective weights, summated together and applied to an activation function in equation (2) to produce a sole output.

$$X = f\left(\sum_{i=0-n} wixi\right) + d \quad (2)$$

Where “ X ” stands for the neuron’s output, “ xi ” for its contribution, “ wi ” for its connecting weights, “ d ” for its bias value, and “ f ” for its initiation function. Feed-forward propagation is used in this study to convey information from contribution nodes. Figure 1 depicts the neural network employed for this investigation.

2.1.3. Comparison parameters

The effects of RSM and ANN models were assessed using a variety of parameters, such as the root mean square error (RMSE), mean absolute error (MAE), coefficient of determination (R^2), coefficient of correlation (R) and mean absolute percentage error (MAPE) [32]. Equations (3)–(5) are used to calculate errors.

Table 1: Levels of variables.

VARIABLES	LOW LEVEL (-1)	HIGH LEVEL (+1)
Ferrocement Volume fraction	0	3.77
Steel slag	0	50

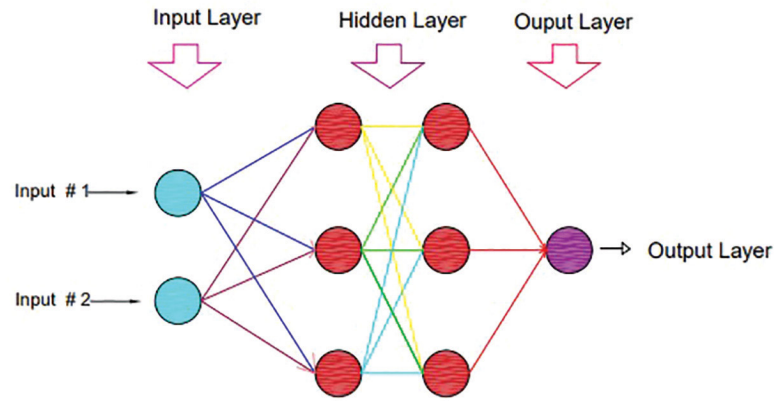


Figure 1: Architecture of ANN.

Table 2: Details of test specimen with chicken mesh for flexure test.

DESIGNATION	VOLUME FRACTION (X_1)	STEEL SLAG (X_2)
1FCGWM	0.94	50
2FCGWM	0.94	0
3FCGWM	3.77	0
4FCGWM	2.355	25
5FCGWM	3.77	50
6FCGWM	2.355	25
7FCGWM	2.355	25
8FCGWM	2.355	0
9FCGWM	0.35	25
10FCGWM	2.355	25
11FCGWM	2.355	60
12FCGWM	2.355	25
13FCGWM	4.35	25

$$\text{RMSE} = \sqrt{\sum_1^n (y-x)^2/n} \quad (3)$$

$$\text{MAE} = \frac{1}{n} \sum_1^n |y-x| \quad (4)$$

$$\text{MAPE} = \sum_1^n |y-x| * 100 \quad (5)$$

Here x = factual data, y = predicted data and n = sample count.

2.2. Materials

For this experiment, Ordinary Portland Cement of 53 grade with a specific gravity of 3.15 and an early setting time of 32 minutes according to IS: 12269-1987 was employed [33]. For ferrocement, river sand with a specific gravity of 2.60 and a size of 2.36 mm is adopted, according to IS: 383-1970 and ACI 549 1R-93, 1999 [34, 35]. According to the guidelines of IS 228 from 1987 [36] steel slag with specific gravity 2.85 passing through 2.36 mm sieve was employed. Chicken mesh with diameter 1.2 mm, spacing 25 mm and tensile strength of 312 N/mm² was used. The ferrocement composites were tested with loads at one third point with a clear span of 400 mm. According to the specifications in Table 2, ferrocement with the dimensions 150 mm × 25 mm × 500 mm was cast and cured with wet burlap.

3. RESULTS AND DISCUSSION

3.1. Experimental investigation

As per to Figure 2, specimens with a V_r of 4.35% and a weight fraction of 25% steel slag achieve an ultimate load of 3.80 kN. For specimens with a volume percentage of 0.35% and a replacement rate of 25% in steel slag, it has been shown that the ultimate load decreases. Also, it is clear that the ultimate load decreases with a lower volume fraction and a higher substitution of steel slag [37].

From Figure 3, it can be shown that specimens with a V_r of 4.35% and 25% steel slag for the fine aggregate attain their extreme moment capacity. It is obvious that the ultimate load and ultimate moment of chicken mesh decreases with decreasing volume fractions. On the other hand, ultimate load and moment capacity rise with greater V_r . The graph makes it obvious that when volume fraction grows, moment capacity also does so due to an increase in moment arm distance and passive confining pressure. Furthermore, the cement matrix and weld mesh are well-anchored, increasing the moment carrying capacity indirectly [37]. It was discovered that the chicken mesh wires were more successful in raising the ultimate load.

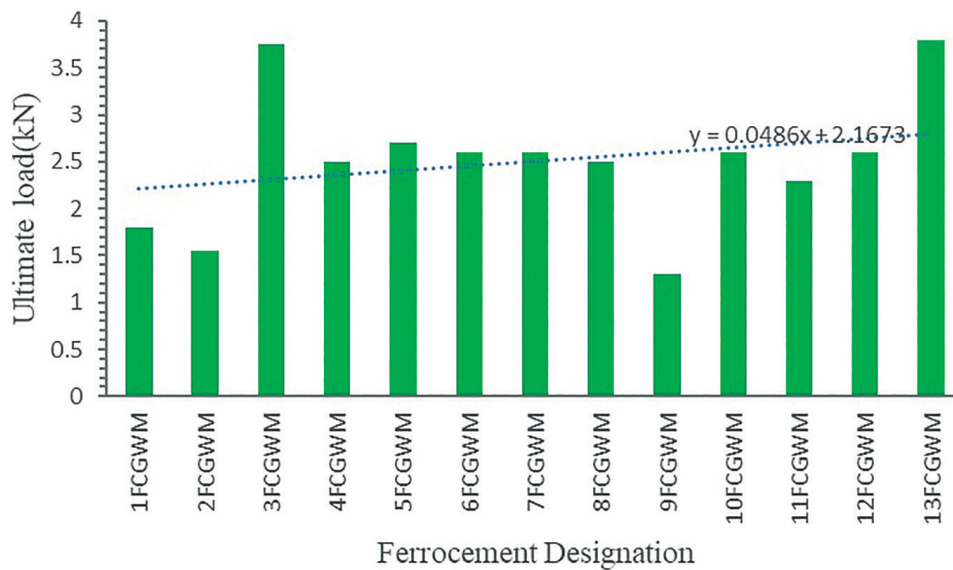


Figure 2: Ultimate load for various replacements of steel slag and the V_r of chicken mesh ferrocement laminates.

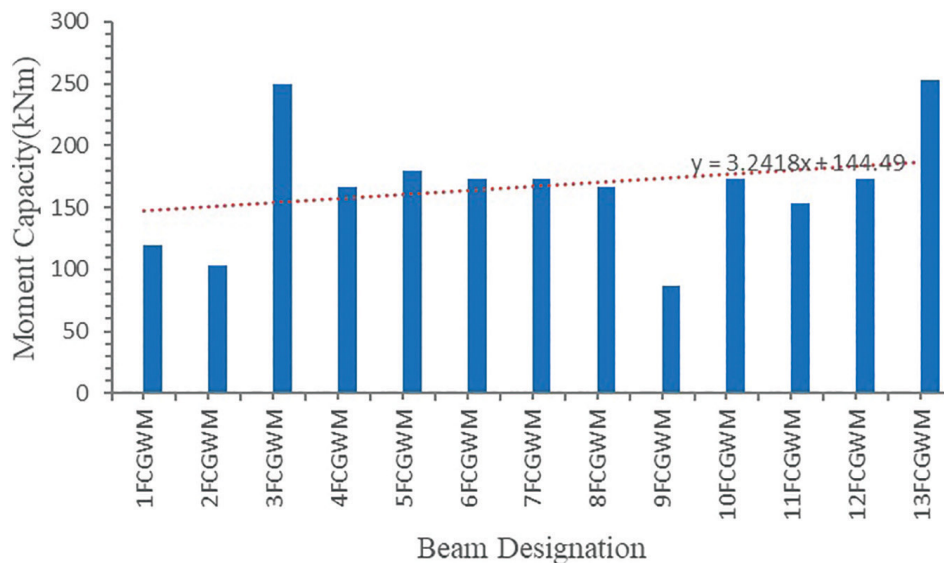


Figure 3: Moment capacity and V_r of weld mesh ferrocement laminates for various steel slag replacements.

3.2. RSM model

According to the CCM, a study was done to determine how the variables V_r and steel slag affected the prediction of the ultimate moment capacity of ferrocement. As arrayed in Table 3, 13 flexure strength trials were carried out, and the results are shown in Table 3. and obtained responses are shown in equations (6).

$$\text{MRS}M = 72.3 + 46.5X_1 + 0.573X_2 + 0.17X_1^2 - 0.00281X_2^2 - 0.422X_1 * X_2 \quad (6)$$

Distribution curve for the MRSM and Normalised plot are shown in Figure 4 and Figure 5. A distribution curve, also known as a probability density function (PDF) or probability distribution curve, is a graphical representation of the probability distribution of a random variable. It provides information about the likelihood of different values occurring for the variable. From Figure 4 bell-shaped curve of the Normal distribution is obtained. In bell curve, the peak represents the most probable event in the dataset while the other events are equally distributed around the peak. Similarly, from Figure 5. From normalized plot for predicting the ultimate moment allows for a relative comparison of different ferrocement laminates.

Table 3: Predicted strengths.

MIX DESIGNATION	VOLUME FRACTION (X_1)	STEEL SLAG (X_2)	ULTIMATE MOMENT (MRS)M) kNmm
1FCGWM	0.94	50	117.95
2FCGWM	0.94	0	116.16
3FCGWM	3.77	0	250.02
4FCGWM	2.355	25	170.47
5FCGWM	3.77	50	192.10
6FCGWM	2.355	25	170.47
7FCGWM	2.355	25	170.47
8FCGWM	2.355	0	186.81
9FCGWM	0.35	25	97.61
10FCGWM	2.355	25	170.47
11FCGWM	2.355	60	147.12
12FCGWM	2.355	25	170.47
13FCGWM	4.35	25	244.70

Note: Where MRSM = ultimate moment, (X_1) = volume fraction and (X_2) = steel slag.

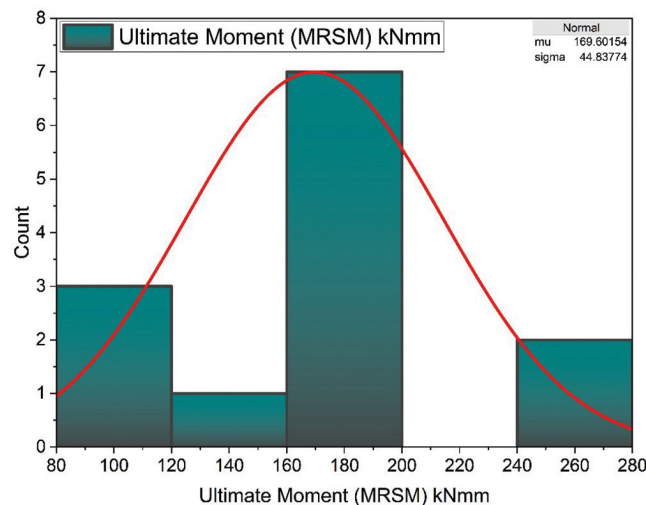


Figure 4: Histogram illustrating bins for the MRSM distribution curve.

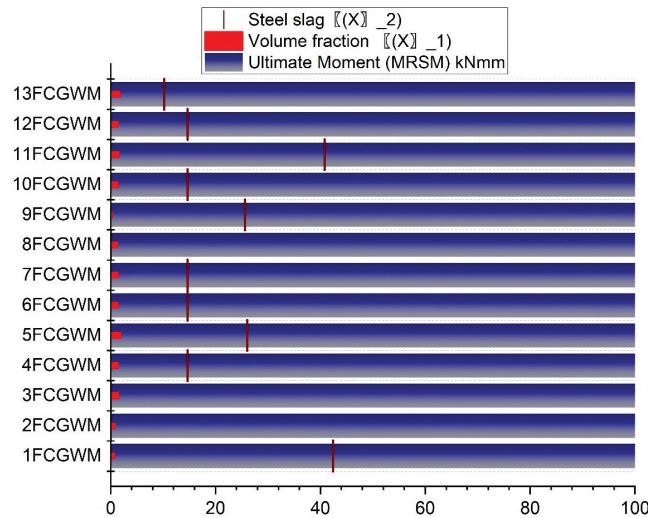


Figure 5: Normalised plot for the values obtained.

3.2.1. P value and pareto analysis

The p value aids in the significance of evolution elements. The p value of the model should be least which is the probability value of the F test, which must be least. The evolution parameters can be significant if its p values are ≤ 0.005 . If the p-value is > 0.005 , it is considered that the progression variable is unimportant. Volume fraction is a significant factor in determining the final moment of ferrocement under flexure, as shown by the fact that X_1 has a lower p-value than X_2 in ANOVA Table 4. Volume fraction is more important than steel slag, as shown by the Pareto chart in Figure 6 since its value was higher when associated to the linear (B) and (AB) lines. The findings are consistent with earlier research, which shows that volume fraction may greatly increase ultimate load and moment capacity [38].

3.2.2. Surface plot analysis

Figure 7 depict three-dimensional (3D), surface plots illustrating the influence of independent variables on the corresponding outcomes. The reaction can be visually depicted through graphical representations in 3D space plots, aiding in the visualization of the response surface's structure [39]. The progression variables, steel slag and volume fraction, are graphed along the “x” and “y” axes, while the response is represented on the “z” axis. In Figure 7a, 3D surface plots were drawn to better understand how independent factors affected the responses. It illustrates the relationship between volume fraction and ultimate moment capacity by showing how the Moment capacity for ferrocement laminates grows as the volume fraction increases from 0.97% to 4.35%. Although the volume fraction is a key component in determining final load and moment capacity, steel slag addition also boosts load bearing capacity when fine aggregate is substituted with steel slag by 25%. From the surface plot, it can be concluded that the V_r of 4.35% and the steel slag content of 25% resulted in the extreme ultimate load and moment capacity. The range of distribution of Moment capacity may be seen in Figure 7b contour plot, which is displayed with self-governing variables volume fraction and steel slag. The graph's response confirms the findings of 3D surface plots.

3.3. ANN Model

Using available data, neural networks (NN) can aid in forecasting the moment capacity of ferrocement when steel slag are introduced. This analysis showcases the forecasted values of moment capacity based on various input steel slag and volume fraction. To validate the NN's predictions, experimental results from ferrocement specimens incorporating individual steel slag and volume fraction are compared with the predicted values. For this investigation Feed-forward back propagation NN-LM training functions are utilised. The results of validation and training are presented in Figure 8. These figures reveals a very strong correlation with $R^2 = 0.98832$ for the training and $R^2 = 0.98412$ for the validation, where R is the linear correlation coefficient. This demonstrates the effectiveness and accuracy of the trained neural network. The results obtained for ferrocement incorporated with weld mesh and steel slag combination are compared with the existing models.

Table 4: Analysis of variance of RSM model.

SOURCE	ULTIMATE MOMENT (MRSM)		
	DF	F-VALUE	P-VALUE
Model	5	37.76	0.000
Linear	2	90.27	0.000
X_1	1	170.24	0.000
X_2	1	10.27	0.015
Square	2	0.06	0.940
X_1^2	1	0.01	0.940
X_2^2	1	0.12	0.743
Two-way Interaction	1	7.03	0.033
$X_1 * X_2$	1	7.03	0.033

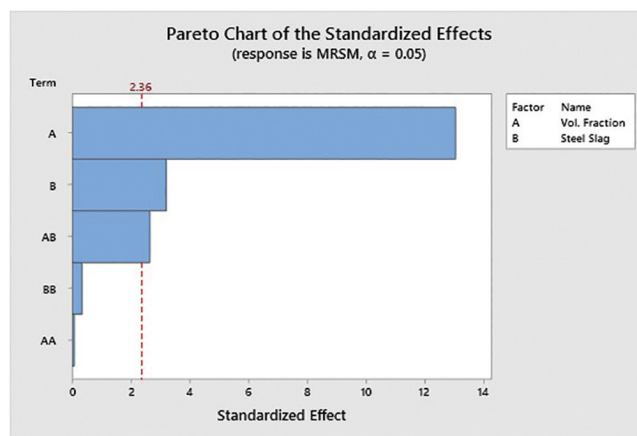


Figure 6: Pareto chart of ultimate moment capacity.

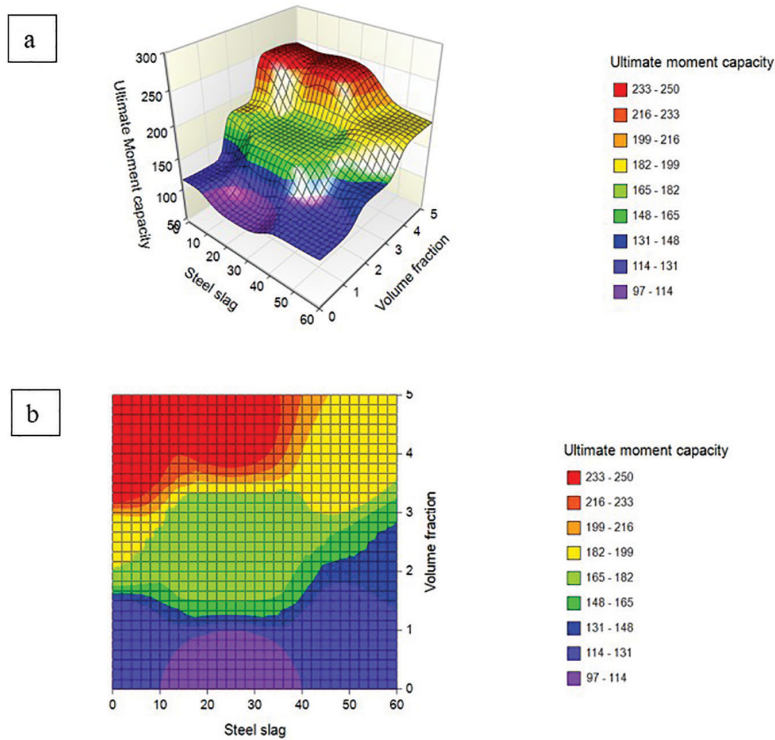


Figure 7: Ultimate moment capacity a) 3D surface plot b) contour plot.

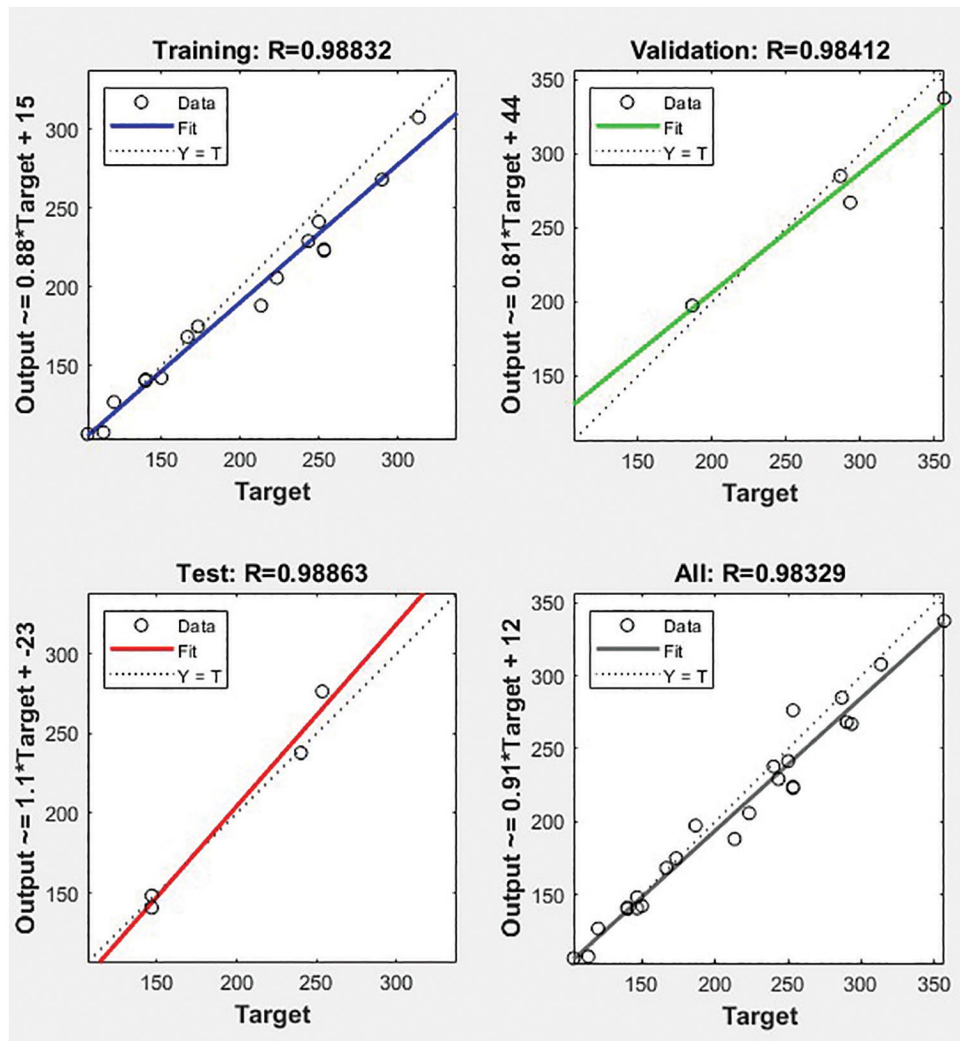


Figure 8: Training and validation of ANN.

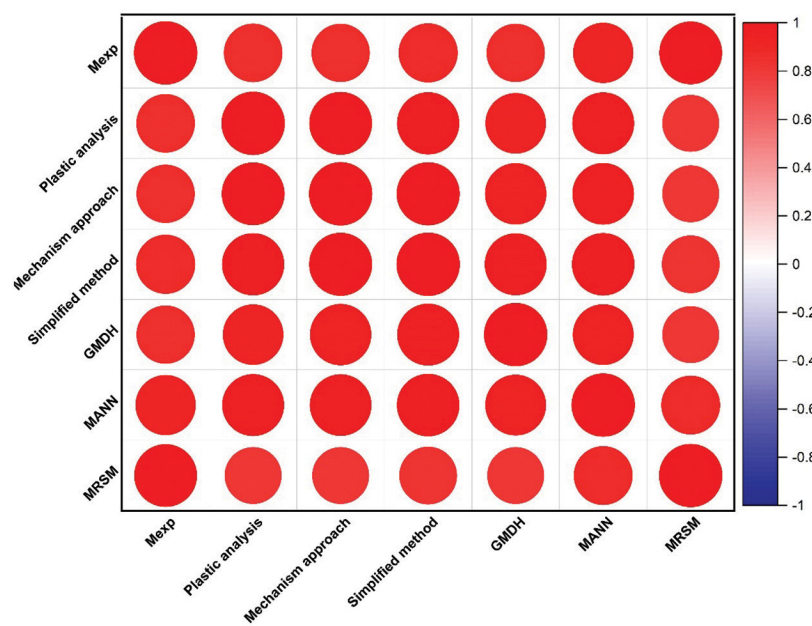


Figure 9: Correlation plot for the values obtained.

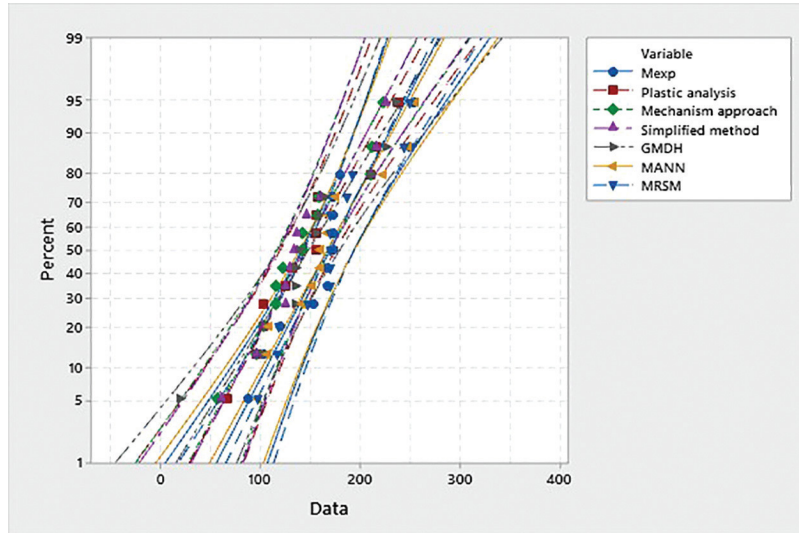


Figure 10: Comparison of experimental results vs different models.

3.4. Comparison of models

The Ultimate moment capacity of experimental and existing theoretical model of ferrocement composites are arrayed in Figure 9 and Figure 10. The outcomes of Back-Propagation Neural Networks, Central Composite Method, Plastic analysis approach, Mechanism approach, Simplified method and GMDH are presented in Table 5 to show the comparison between theoretical models and experimental results. Assessed results of ANN and RSM are related with the plastic analysis, Mechanism approach, Simplified method and GMDH in Figure 9 and Figure 10. When comparing the performance of all the models, it appears that ANN and RSM outperforms other models currently in use. From the table it clear that in irrespective of the model maximum moment capacity for ferrocement is gained for 13FCGWM which has volume fraction of 4.35% and steel slag replacement of 25%.

Table 5: Comparison of ultimate moment capacity.

TEST.NO.	M_{exp}	PLASTIC ANALYSIS $\text{Mu} = \sigma_{tu} \times \frac{b(h - X_1)h}{2}$ [40]	MECHANISM APPROACH $\text{Mu} = \sigma_{tu} \times \frac{bh^2}{2}$ [41]	SIMPLIFIED METHOD $y = -0.0772x^2 + 0.422x + 0.005$ $x = \frac{v_f \sigma_y}{f'}$ $y = \frac{\text{Mu}}{\eta_0 f'_c \cdot bh^2}$ [42]	GROUP METHOD OF DATA HANDLING $\text{Mu} = 0.091 + \frac{0.009hf'_{cu}}{b} - \frac{0.042h^2}{v_f} + \frac{bw_f(10.37h^2 f'_{ul} - 0.021v_f)}{f'_{ul}}$ [17]	MANN (kNmm)	MRSM (kNmm)
1FCGWM	120.00	95.56	96.27	96.12	102.12	106.65	117.95
2FCGWM	103.33	102.12	102.56	103.25	105.56	107.76	116.16
3FCGWM	250.00	215.56	212.56	225.56	235.58	248.40	250.02
4FCGWM	166.67	132.25	115.56	125.56	156.58	168.42	170.47
5FCGWM	180.00	102.23	115.58	125.56	135.52	141.35	192.10
6FCGWM	173.33	125.56	122.13	129.12	138.89	167.01	170.47
7FCGWM	173.33	156.58	141.23	135.89	158.89	160.40	170.47
8FCGWM	166.67	156.56	142.23	132.88	135.58	152.37	186.81
9FCGWM	86.67	66.25	56.58	60.28	18.89	97.45	97.61
10FCGWM	173.33	210.23	209.89	210.00	225.56	223.12	170.47
11FCGWM	153.33	156.58	158.89	160.25	164.56	175.00	147.12
12FCGWM	173.33	156.68	157.25	145.58	135.56	160.80	170.47
13FCGWM	253.33	238.25	222.56	215.48	210.56	255.88	244.70

Table 6: Assessment of existing models with RSM and ANN.

STATISTICAL PARAMETER	M_{exp}	PLASTIC ANALYSIS	MECHANISM APPROACH	SIMPLIFIED METHOD	GMDH	MANN	MRSM
Mean	210.7	204.5	200.7	198.6	202.7	203.6	204.6
Standard deviation	70.7	75.6	75.7	73.2	68.6	65.4	65.6
RSME	0.48	0.0932	0.0889	0.1586	0.0365	0.0352	0.0356
MAPE	13.25%	12.58%	13.58%	14.58%	13.45%	11.56%	12.01%
MAE	0.04	0.0358	0.0445	0.0892	0.0156	0.0125	0.0132
Correlation (R)	0.9667	0.9235	0.8785	0.8568	0.9786	0.9886	0.9643

Where

h = Thickness of the ferrocement member, b = Breadth of the ferrocement member, x_1 = Depth of the neutral axis, f_{cu} = strength of mortar under compression, f_u = Ultimate tensile strength chicken mesh, A_s = Area of steel, $\sigma_{tu} = \frac{A_s f_u}{bh}$, νf = Volume fraction of chicken, η_0 = Global efficiency factor of chicken mesh, σ_y = Yield tensile strength of chicken mesh, f'_c = strength of mortar under compression.

Equations (7)–(9) demonstrate how RMSE, MAPE, and MAE are adopted to assess the model's performance with the pre-existing models. As per the statistical outcomes shown in Table 6, ANN and RSM presented in this study have good evaluation performance when compared to the existing models projected. The estimated error values of Root Mean Square Error (RMSE) of the ANN proposed is lesser than the other models considered. The MAPE and MAE was found to be minimum for MANN for the coefficient of detection (R^2) for the ANN and RSM is 98% and 96% respectively.

$$RMSE = \sqrt{\frac{1}{n} \sum_{i=1}^n (\text{Mu(actual)} - \text{Mu(model)})^2} \quad (7)$$

$$MAPE = \frac{1}{n} \left(\sum_{i=1}^n \frac{|\text{Mu(actual)} - \text{Mu(model)}|}{(\text{Mu(actual)})} \right) \times 100 \quad (8)$$

$$MAE = \frac{1}{n} \left(\sum_{i=1}^n (|\text{Mu(actual)} - \text{Mu(model)}|) \right) \quad (9)$$

4. CONCLUSION

In the current work, the ultimate moment capacity of ferrocement composites containing steel slag in varying volumes is determined using ANN and RSM, and the findings are outlined below.

- The Ultimate Moment capacity of ferrocement laminates has increased for ferrocement with 4.35% and 25% by weight of steel slag as fine aggregate.
- The ANNOVA outcomes indicate that the volume percentage of mesh reinforcement is the major indicator of ultimate moment capacity.
- The RSM model for Moment capacity were shown to be very significant by Analysis of Variance and Pareto chart analysis. Because the models' p values were less than 0.005, their mathematical outputs were very precise. The volume fraction (X_1) was discovered to be the most important factor for ultimate Moment capacity.
- The chosen Leven Berg-Marquardt (NN-LM) and Feed-forward back propagation neural network has a regression value of 0.9882 and 0.98863 for training and testing respectively. The comparative results with different studies clearly indicate that the projected ANN model and RSM model has a high level of accuracy which can be used for prediction of the ultimate moment of ferrocement composites. Additionally, findings indicate that the V_r of chicken mesh is crucial for ferrocement composites' ultimate moment capacity.

- Ferrocement composites with 4.35% steel slag content find applications in lightweight construction panels, architectural cladding, and decorative elements, offering a balanced combination of structural strength and reduced weight. These laminates are suitable for non-load-bearing elements and aesthetic applications where versatility and design flexibility are crucial.

5. BIBLIOGRAPHY

- [1] INTERNATIONAL FERROCEMENT SOCIETY, *Ferrocement model code: building code recommendations for the ferrocement: Reported by IFS Committee 10 (IFS 10-01)*, Klong Luang, International Ferrocement Society, 2001.
- [2] HANAZADI, M.K., RAMESHT, M.H., “The effect of cover and arrangement of reinforcement on the behaviour of ferrocement in tension”, *Journal of Ferrocement*, v. 26, n. 2, pp. 85–94, 1996.
- [3] NAAMAN, A.E., *Ferrocement and laminated cementitious composites*, Michigan, USA, Techno Press 3000, 2000.
- [4] SHEELA, S., GANESAN, N., “Flexural behaviour of polymer modified ferrocement elements with different types of fine aggregates”, *Journal of Ferrocement*, v. 35, n. 2, pp. 541–558, 2005.
- [5] ESKANDARI, H., MADADI, A., “Investigation of ferrocement channels using experimental and finite element analysis”, *Engineering Science and Technology International Journal*, v. 18, n. 4, pp. 769–775, 2015.
- [6] JEEVA, C.S., KUMAR, S., “Flexural behaviour of bamboo based ferrocement slab panels with fly ash”, *Construction & Building Materials*, v. 134, pp. 641–648, 2017. doi: <http://dx.doi.org/10.1016/j.conbuildmat.2016.12.205>.
- [7] SHAABAN, I.G., SHAHEEN, Y.B., ELSAYED, E.L., *et al.*, “Flexural behaviour and theoretical prediction of lightweight ferrocement composite beams”, *Case Studies in Construction and Building Materials*, v. 9, pp. 1–17, 2018. doi: <http://dx.doi.org/10.1016/j.cscm.2018.e00204>.
- [8] MUGHAL, U.A., SALEEM, M.A., ABBAS, S., “Comparative study of ferrocement panels reinforced with galvanized iron and polypropylene meshes”, *Construction & Building Materials*, v. 210, pp. 40–47, 2019. doi: <http://dx.doi.org/10.1016/j.conbuildmat.2019.03.147>.
- [9] JAYAPRAKASH, S., DHANAPAL, J., DEIVASIGAMANI, V., *et al.*, “Flexural behaviour of chicken mesh ferrocement laminates with partial replacement of fine aggregate by steel slag. advances in material science and engineering”, *Advances in Materials Science and Engineering*, v. 21, pp. 1–9, 2021. doi: <http://dx.doi.org/10.1155/2021/7307493>.
- [10] SRIDHAR, J., MALATHY, R., “Effect of industrial waste-steel slag in Impact behaviour of ferrocement panel”, *Ecology Environment and Conservation*, v. 23, n. 3, pp. 1709–1715, 2017.
- [11] SANKAR, K., SHOBA RAJKUMAR, D., “Experimental investigation on different high rich cement mortar for ferrocement application”, *Materials Today: Proceedings*, v. 22, pp. 858–864, 2019. doi: <http://dx.doi.org/10.1016/j.matpr.2019.11.033>.
- [12] QESHTA, I.M.I., SHAFIGH, P., JUMAAT, M.Z., *et al.*, “The use of wire mesh-epoxy composite for enhancing the flexural performance of concrete beams”, *Materials & Design*, v. 60, pp. 250–259, 2014. doi: <http://dx.doi.org/10.1016/j.matdes.2014.03.075>.
- [13] ZHANG, K., SUN, Q., “The use of Wire Mesh-Polyurethane Cement (WM-PUC) composite to strengthen RC T-beams under flexure”, *Journal of Building Engineering*, v. 15, pp. 122–136, 2018. doi: <http://dx.doi.org/10.1016/j.jobbe.2017.11.008>.
- [14] CHEAH, C.B., RAMLI, M., “Load capacity and crack development characteristics of HCWA-DSF high strength mortar ferrocement panels in flexure”, *Construction & Building Materials*, v. 36, pp. 348–357, 2012. doi: <http://dx.doi.org/10.1016/j.conbuildmat.2012.05.034>.
- [15] MADADI, A., ESKANDARI-NADDAF, H., SHADNIA, R., *et al.*, “Characterization of ferrocement slab panels containing lightweight expanded clay aggregate using digital image correlation technique”, *Construction & Building Materials*, v. 180, pp. 464–476, 2018. doi: <http://dx.doi.org/10.1016/j.conbuildmat.2018.06.024>.
- [16] ISMAIL, A., “Estimating moment capacity of ferrocement members using self-evolving network”, *Frontiers of Structural and Civil Engineering*, v. 13, n. 4, pp. 926–936, 2019. doi: <http://dx.doi.org/10.1007/s11709-019-0527-5>.

- [17] NADERPOUR, H., EIDGAHEE, D.R., FAKHARIAN, P., *et al.*, “A new proposed approach for moment capacity estimation of ferrocement members using Group Method of Data Handling”, *Engineering Science and Technology International Journal*, v. 23, n. 2, pp. 382–391, 2020.
- [18] SIPOS, TK, PARSA, P., “Empirical formulation of ferrocement members moment capacity using artificial neural networks”, *Journal of Soft Computing in Civil Engineering*, v. 4, n. 1, pp. 111–126, 2020. doi: <http://dx.doi.org/10.22115/SCCE.2020.221268.1181>.
- [19] SAMSON JEROLD SAMUEL, C., RAMESH, A., “Investigation on microstructure and tensile behaviour of stir cast LM13 Aluminium alloy reinforced with copper coated short steel fibres using response surface methodology”, *Transactions of the Indian Institute of Metals*, v. 71, n. 9, pp. 2221–2230, 2018. doi: <http://dx.doi.org/10.1007/s12666-018-1353-5>.
- [20] HAMMOUDI, A., MOUSSACEB, K., BELEBCHOUCHE, C., *et al.*, “Comparison of artificial neural network (ANN) and response surface methodology (RSM) prediction in compressive strength of recycled concrete aggregates”, *Construction & Building Materials*, v. 209, pp. 425–436, 2019. doi: <http://dx.doi.org/10.1016/j.conbuildmat.2019.03.119>.
- [21] MOODI, Y., MOUSAVI, S.R., GHAVIDEL, A., *et al.*, “Using response surface methodology and providing a modified model using whale algorithm for estimating the compressive strength of columns confined with FRP sheets”, *Construction & Building Materials*, v. 183, pp. 163–170, 2018. doi: <http://dx.doi.org/10.1016/j.conbuildmat.2018.06.081>.
- [22] SAMSON JEROLD SAMUEL, C., RAMESH, A., “Dry sliding wear characterization of squeeze cast LM13/FeCu composite using response surface methodology”, *China Foundry*, v. 14, n. 6, pp. 525–533, 2017. doi: <http://dx.doi.org/10.1007/s41230-017-7101-3>.
- [23] AZIMINEZHAD, M., MAHDIKHANI, M., MEMARPOUR, M.M., “RSM-based modeling and optimization of self-consolidating mortar to predict acceptable ranges of rheological properties”, *Construction & Building Materials*, v. 189, pp. 1200–1213, 2018. doi: <http://dx.doi.org/10.1016/j.conbuildmat.2018.09.019>.
- [24] VAF AEI, A., GHAEDI, A.M., AVAZZADEH, Z., *et al.*, “Removal of hydrochlorothiazide from molecular liquids using carbon nanotubes: radial basis function neural network modeling and culture algorithm optimization”, *Journal of Molecular Liquids*, v. 324, pp. 114766, 2021. doi: <http://dx.doi.org/10.1016/j.molliq.2020.114766>.
- [25] RAJU, U., “2023, Prediction of strength properties of concrete with jute fibres, kenaf fibers and silica fumes: a response surface methodology (DOE) approach”, *Matéria (Rio de Janeiro)*, v. 28, n. 4, pp. e20230235, 2023. doi: <http://dx.doi.org/10.1590/1517-7076-rmat-2023-0235>.
- [26] MUTHUKUMAR, S.R., JEGATHEESWARAN., “Prediction of autoclaved aerated cement block masonry prism strength under compression using machine learning tools”, *Matéria (Rio de Janeiro)*, v. 29, n. 1, pp. e20230247, 2024. doi: <http://dx.doi.org/10.1590/1517-7076-rmat-2023-0247>.
- [27] WANG, W., CHENG, Y., TAN, G., “Design Optimization of SBS-modified asphalt mixture reinforced with eco-friendly basalt fiber based on response surface methodology”, *Materials (Basel)*, v. 11, n. 8, pp. 1–22, 2018. doi: <http://dx.doi.org/10.3390/ma11081311>. PubMed PMID: 30060603.
- [28] ARUMUGAM, S., SRIRAM, G., RAJMOHAN, T., “Multi-response optimization of epoxidation process parameters of rapeseed oil using response surface methodology (RSM)-based desirability analysis”, *Arabian Journal for Science and Engineering*, v. 39, n. 3, pp. 2277–2287, 2012. doi: <http://dx.doi.org/10.1007/s13369-013-0789-5>.
- [29] BALACHANDRAN, M., DEVANATHAN, S., MURALEEKRISHNAN, R., *et al.*, “Optimizing properties of Nanoclay-nitrile rubber (NBR) composites using Face Centred Central Composite Design”, *Materials & Design*, v. 35, pp. 854–862, 2012. doi: <http://dx.doi.org/10.1016/j.matdes.2011.03.077>.
- [30] SRIDHAR, J., VIVEK, D., “Influence of non-biodegradable wastes in mechanical properties of concrete: a neural network approach”, *IOP Conference Series. Materials Science and Engineering*, v. 1025, n. 1, pp. 1–9, 2021. doi: <http://dx.doi.org/10.1088/1757-899X/1025/1/012007>.
- [31] DHANAPAL, J., JEYAPRAKASH, S., “Mechanical properties of mixed steel fiber reinforced concrete with the combination of micro and macro steel fibers”, *Structural Concrete*, v. 21, n. 1, pp. 458–467, 2020. doi: <http://dx.doi.org/10.1002/suco.201700219>.
- [32] BHOWMIK, M., DEB, K., DEBNATH, A., *et al.*, “Mixed phase Fe₂O₃/Mn₃O₄ magnetic nanocomposite for enhanced adsorption of methyl orange dye: Neural network modeling and response surface methodology optimization”, *Applied Organometallic Chemistry*, v. 32, n. 3, pp. e4186, 2018. doi: <http://dx.doi.org/10.1002/aoc.4186>.

- [33] BUREAU OF INDIAN STANDARDS, *IS:12269: specifications for 53 grade ordinary portland cement*, New Delhi, BIS, 1987.
- [34] BUREAU OF INDIAN STANDARDS, *IS:383: specifications for coarse and fine aggregates from natural sources for concrete*, New Delhi, BIS, 1970.
- [35] AMERICAN CONCRETE INSTITUTE, *ACI 549.1R-93: guide for the design, construction and repair of ferrocement*, Farmington Hills, ACI Committee, 1999.
- [36] BUREAU OF INDIAN STANDARDS, *IS 228: method of chemical analysis of steels*, New Delhi, BIS, 1987
- [37] SRIDHAR, J., MALATHY, R., “Behaviour of ferrocement laminates with industrial waste-steel slag under flexure”, *Ecology Environment and Conservation*, v. 2018, pp. S441–S449, 2018.
- [38] SRIDHAR, J., SHINDE, G.B., VIVEK, D., *et al.*, “Response surface methodology approach to predict the flexural moment of ferrocement composites with weld mesh and steel slag as partial replacement for fine aggregate”, *Advances in Materials Science and Engineering*, v. 2022, pp. 1–9, 2022. doi: <http://dx.doi.org/10.1155/2022/9179480>.
- [39] MOMTAZAN, F., VAFAEI, A., GHAEDI, M., *et al.*, “Application of copper sulfide nanoparticles loaded activated carbon for simultaneous adsorption of ternary dyes: response surface methodology”, *Korean Journal of Chemical Engineering*, v. 35, n. 5, pp. 1108–1118, 2018. doi: <http://dx.doi.org/10.1007/s11814-018-0012-1>.
- [40] MANSUR, M., PARAMASIVAM, P., “Cracking behavior and ultimate strength of ferrocement in flexure”, *Journal of Ferrocement*, v. 16, pp. 405–415, 1986.
- [41] PARAMASIVAM, P., RAVINDRARAJAH, R., “Effect of arrangements of reinforcements on mechanical properties of ferrocement”, *ACI Structural Journal*, v. 85, pp. 3–11, 1988.
- [42] NAAMAN, A., “Flexural design of ferrocement: computerized evaluation and design aids”, *Journal of Ferrocement*, v. 16, pp. 101–116, 1986.